arXiv:1208.2992v1 [math-ph] 14 Aug 2012

CRITICAL PHENOMENA IN EXPONENTIAL RANDOM GRAPHS

MEI YIN

August 14, 2012

Abstract. The exponential family of random graphs is among the most promising class of network models. Dependence between the random edges is defined through certain finite subgraphs, in imitation of the use of potential energy to provide dependence between particle states in a grand canonical ensemble of statistical physics. By adjusting the specific values of these subgraph densities, one could analyze the influence of various local features on the global structure of the network. Loosely put, a phase transition occurs when a singularity arises in the limiting free energy density, as it is the generating function for the limiting expectations of all thermodynamic observables. We derive the full phase diagram for a large family of 3-parameter exponential random graph models with attraction and show that they all consist of a first order surface phase transition bordered by a second order critical curve.

1. Introduction

The exponential family of random graphs is one of the most widely studied network models. Their popularity lies in the fact that they capture a wide variety of common network tendencies, such as connectivity and reciprocity, by representing a complex global structure through a set of tractable local features. The theoretical foundations for these models were originally laid by Besag [1], who applied methods of statistical analysis and demonstrated the powerful Markov-Gibbs equivalence (Hammersley-Clifford theorem [2]) in the context of spatial data. Building on Besag's work, further investigations quickly followed. Holland and Leinhardt [3] derived the exponential family of distributions for networks in the directed case. Frank and Strauss [4] showed that the random graph edges form a Markov random field when the local network features are given by counts of various triangles and stars. Newer developments are summarized in Snijders et al. [5] and Rinaldo et al. [6]. (See Wasserman and Faust [7] for a comprehensive review of the methods and models for analyzing network properties.)

As usual in statistical physics, we start with a finite probability space, namely the set $\mathcal{G}_n$ of all simple graphs on n vertices ("simple" means undirected, with no loops or multiple edges). The general k-parameter family of exponential random graphs is defined by assigning a probability mass function $\mathbb{P}_n^\beta(G_n)$ to every simple graph $G_n \in \mathcal{G}_n$:

$$\mathbb{P}_n^\beta(G_n) = \exp\left(n^2(\beta_1 t(H_1, G_n) + \cdots + \beta_k t(H_k, G_n) - \psi_n^\beta)\right), \tag{1}$$

where $\beta = (\beta_1, ..., \beta_k)$ are k real parameters, $H_1, ..., H_k$ are pre-chosen finite simple graphs (in particular, H_1 is a single edge), $t(H_i, G_n)$ is the density of graph homomorphisms (the probability that a random vertex map $V(H_i) \to V(G_n)$ is edge-preserving),

$$t(H_i, G_n) = \frac{|\hom(H_i, G_n)|}{|V(G_n)|^{|V(H_i)|}}, \tag{2}$$

and ψ_n^β is the normalization constant (free energy density), i.e., it satisfies

$$\sum_{G_n \in \mathcal{G}_n} \exp\left(n^2\left(\beta_1 t(H_1, G_n) + \cdots + \beta_k t(H_k, G_n)\right)\right) = \exp\left(n^2 \psi_n^\beta\right). \tag{3}$$

Since real-world networks are often very large in size, ranging from hundreds to billions of vertices, our main interest will be in the behavior of the exponential random graph G_n in the large n limit. Intuitively, the k parameters $\beta_1, ..., \beta_k$ allow one to adjust the influence of different local features (in this case, densities of different subgraphs $H_1, ..., H_k$) on the limiting probability distribution, and a natural question to ask is how would the tuning of parameters impact the global structure of a typical random graph G_n drawn from this model? Loosely put, a phase transition occurs when the limiting free energy density $\psi_\infty^\beta = \lim_{n\to\infty} \psi_n^\beta$ has a singular point. The reason behind this is that the limiting free energy density is the generating function for the limiting expectations of all thermodynamic observables (see for instance [8]),

$$\lim_{n\to\infty} \mathbb{E}^\beta t(H_i, G_n) = \lim_{n\to\infty} \frac{\partial}{\partial \beta_i} \psi_n^\beta = \frac{\partial}{\partial \beta_i} \psi_\infty^\beta, \tag{4}$$

$$\lim_{n\to\infty} n^2 \left(\mathbb{C}\mathrm{ov}^\beta\left(t(H_i, G_n), t(H_j, G_n)\right)\right) = \lim_{n\to\infty} \frac{\partial^2}{\partial \beta_i \partial \beta_j} \psi_n^\beta = \frac{\partial^2}{\partial \beta_i \partial \beta_j} \psi_\infty^\beta, \tag{5}$$

so a singularity in the limiting thermodynamic function must arise from a singularity in the limiting free energy density.

Definition 1.1. *A phase is a connected region of the parameter space $\{\beta\}$, maximal for the condition that the limiting free energy density ψ_∞^β is analytic. There is a jth-order transition at a boundary point of a phase if at least one jth-order partial derivative of ψ_∞^β is discontinuous there, while all lower order derivatives are continuous.*

For $k = 1$, it has been well established that the exponential model is equivalent to the famous Erdős-Rényi random graph $G(n, \rho)$ [9], and its structure is completely specified by the edge formation probability $\rho = e^{2\beta_1}/(1 + e^{2\beta_1})$. As ρ increases, the model displays a sharp phase transition: From a low-density state in which there are few edges to a high-density state in which an extensive fraction of all vertices are joined together in a single giant component.

For $k = 2$, the situation is understandably more complicated and has attracted enormous attention in recent years: Park and Newman [10] [11] developed mean-field approximations and analyzed the phase diagram for the edge-2-star and edge-triangle models. Chatterjee and Diaconis [12] gave the first rigorous proof of singular behavior in the edge-triangle model with the help of the emerging tools of graph limits as developed by Lovász and coworkers [13]. There are also related results in Häggström and Jonasson [14] and Bhamidi et al. [15]. Radin and Yin [16] derived the full phase diagram for 2-parameter exponential random graph models with attraction ($\beta_2 \geq 0$) and showed that they all contain a first order transition curve ending in a second order critical point. Aristoff and Radin [17] treated 2-parameter random graph models with repulsion ($\beta_2 \leq 0$) and proved that the region of parameter space corresponding to multipartite structure is separated by a phase transition from the region of disordered graphs (their proof was recently improved by Yin).

One of the key motivations for considering exponential random graphs is to develop models that exhibit transitivity and clumping (i.e., a friend of a friend is likely also a friend). However, as seen in experiments and through heuristics [11], it is often futile to model transitivity with only 2 subgraphs H_1 and H_2 as sufficient statistics. To get around this problem, more local features of the random graph G_n need to be captured [12]. We therefore incorporate the density of one more subgraph H_3 into the probability distribution and study the phase structure of the exponential model in the $k=3$ setting. Our main results are the following.

Theorem 1.2. *Consider a 3-parameter exponential random graph model (1). Assume H_2 has p edges and H_3 has q edges with $2 \leq p \leq q \leq 5p-1$. Then the limiting free energy density ψ_∞^β exists at all $\{(\beta_1, \beta_2, \beta_3) : \beta_2 \geq 0, \beta_3 \geq 0\}$, and is analytic except on a certain continuous surface S which includes three bounding curves C_1, C_2, and C_3: The surface S approaches the plane $\beta_1+\beta_2+\beta_3=0$ as $\beta_1 \to -\infty$, $\beta_2 \to \infty$, and $\beta_3 \to \infty$; The curve C_1 is the intersection of S with the (β_1, β_2) plane $\{(\beta_1, \beta_2, \beta_3) : \beta_3 = 0\}$; The curve C_2 is the intersection of S with the (β_1, β_3) plane $\{(\beta_1, \beta_2, \beta_3) : \beta_2 = 0\}$; The curve C_3 is a critical curve, and is given parametrically by*

$$\begin{aligned}
\beta_1(u) &= \frac{1}{2}\log\frac{u}{1-u} - \frac{1}{2(p-1)(1-u)} + \frac{pu-(p-1)}{2(p-1)(q-1)(1-u)^2},\\
\beta_2(u) &= \frac{qu-(q-1)}{2p(p-1)(p-q)u^{p-1}(1-u)^2},\\
\beta_3(u) &= \frac{pu-(p-1)}{2q(q-1)(q-p)u^{q-1}(1-u)^2},
\end{aligned} \tag{6}$$

where we take $\frac{p-1}{p} \leq u \leq \frac{q-1}{q}$ to meet the non-negativity constraints on β_2 and β_3 (see Figure 1). All the first derivatives $\frac{\partial}{\partial \beta_1}\psi_\infty^\beta$, $\frac{\partial}{\partial \beta_2}\psi_\infty^\beta$, and $\frac{\partial}{\partial \beta_3}\psi_\infty^\beta$ have (jump) discontinuities across the surface S, except along the curve C_3 where, however, all the second derivatives $\frac{\partial^2}{\partial \beta_1^2}\psi_\infty^\beta$, $\frac{\partial^2}{\partial \beta_2^2}\psi_\infty^\beta$, $\frac{\partial^2}{\partial \beta_3^2}\psi_\infty^\beta$, $\frac{\partial^2}{\partial \beta_1 \partial \beta_2}\psi_\infty^\beta$, $\frac{\partial^2}{\partial \beta_1 \partial \beta_3}\psi_\infty^\beta$, and $\frac{\partial^2}{\partial \beta_2 \partial \beta_3}\psi_\infty^\beta$ diverge.

Corollary 1.3. *The parameter space $\{(\beta_1, \beta_2, \beta_3) : \beta_2 \geq 0, \beta_3 \geq 0\}$ consists of a single phase with a first order phase transition across the surface S and a second order phase transition along the critical curve C_3.*

To derive these results, we will make use of two theorems from [12], which connect the occurrence of a phase transition in our model with the solution of a certain maximization problem (a more extensive explanation may be found in [13]).

Theorem 1.4 (Theorem 4.1 in [12])**.** *Consider a general k-parameter exponential random graph model (1). Suppose $\beta_2, ..., \beta_k$ are non-negative. Then the limiting free energy density ψ_∞^β exists, and is given by*

$$\psi_\infty^\beta = \sup_{0 \leq u \leq 1}\left(\beta_1 u^{E(H_1)} + \cdots + \beta_k u^{E(H_k)} - \frac{1}{2}u\log u - \frac{1}{2}(1-u)\log(1-u)\right), \tag{7}$$

where $E(H_i)$ is the number of edges in H_i.

Theorem 1.5 (Theorem 4.2 in [12])**.** *Let G_n be an exponential random graph drawn from (1). Suppose $\beta_2, ..., \beta_k$ are non-negative. Then G_n behaves like an Erdős-Rényi graph $G(n, u^*)$ in the large n limit, where u^* is picked randomly from the set U of maximizers of (7).*

The rest of this paper is organized as follows. In Section 2 we analyze the maximization problem (7) for $k=3$ in detail (Proposition 2.1) and describe the transition surface S and the bounding curves C_1, C_2, and C_3 explicitly (Proposition 2.3). In Section 3 we investigate the analyticity properties of the limiting free energy density ψ_∞^β in different parameter regions (Theorems 3.1 and 3.3) and complete the proof of our main theorem (Theorem 1.2).

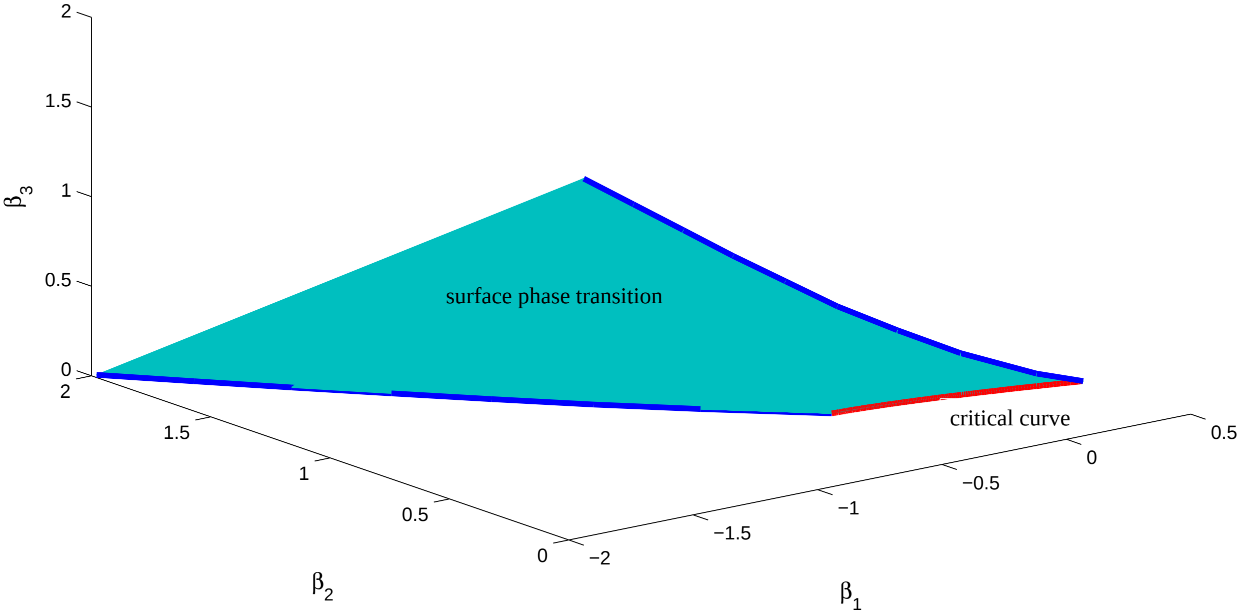

FIGURE 1. Phase transition surface S and critical curve C_3. Graph drawn for $p=3$ and $q=5$.

2. MAXIMIZATION ANALYSIS

Proposition 2.1. *Fix β_3 and integers p and q with $2 \leq p \leq q \leq 5p-1$. Consider the maximization problem for*

$$l_{\beta_3}(u;\beta_1,\beta_2) = \beta_1 u + \beta_2 u^p + \beta_3 u^q - \frac{1}{2}u\log u - \frac{1}{2}(1-u)\log(1-u) \tag{8}$$

on the interval $[0,1]$, where $-\infty < \beta_1 < \infty$ and $-\infty < \beta_2 < \infty$ are parameters. Then there is a V-shaped region in the (β_1,β_2) plane with corner point (β_1^c,β_2^c),

$$\begin{aligned} \beta_1^c &= \frac{1}{2}\log\frac{u_0}{1-u_0} - \frac{1}{2(p-1)(1-u_0)} + \frac{pu_0-(p-1)}{2(p-1)(q-1)(1-u_0)^2}, \\ \beta_2^c &= \frac{qu_0-(q-1)}{2p(p-1)(p-q)u_0^{p-1}(1-u_0)^2}, \end{aligned} \tag{9}$$

where u_0 is uniquely determined by

$$\beta_3 = \frac{pu_0-(p-1)}{2q(q-1)(q-p)u_0^{q-1}(1-u_0)^2}. \tag{10}$$

Outside this region, $l_{\beta_3}(u)$ has only one local maximizer (hence global maximizer) u^*; Inside this region, $l_{\beta_3}(u)$ has exactly two local maximizers u_1^* and u_2^*. For every β_1 inside this V-shaped region ($\beta_1 < \beta_1^c$), there is a unique decreasing $\beta_2 = r_{\beta_3}(\beta_1)$ such that u_1^* and u_2^* are both global maximizers for $l_{\beta_3}(u;\beta_1,r_{\beta_3}(\beta_1))$ (see Figures 2 and 3).

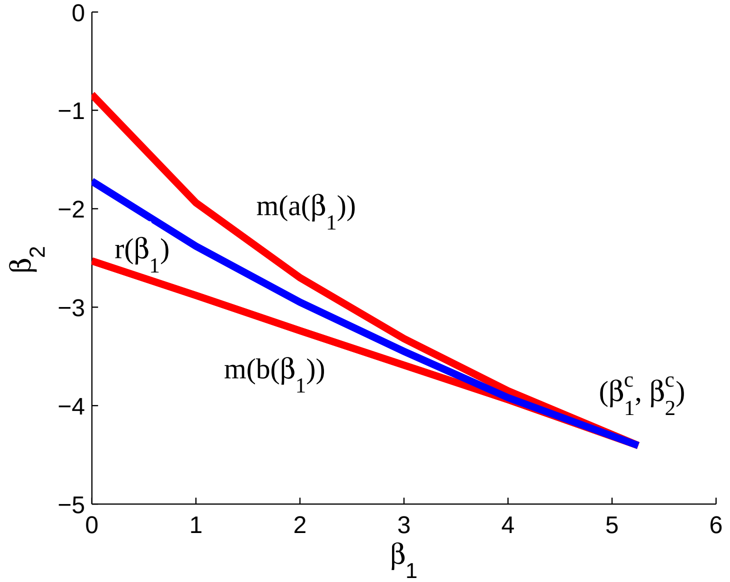

FIGURE 2. The V-shaped region (with phase transition curve $r(\beta_1)$ inside) in the (β_1, β_2) plane. Graph drawn for $\beta_3 = 2$, $p = 3$, and $q = 5$.

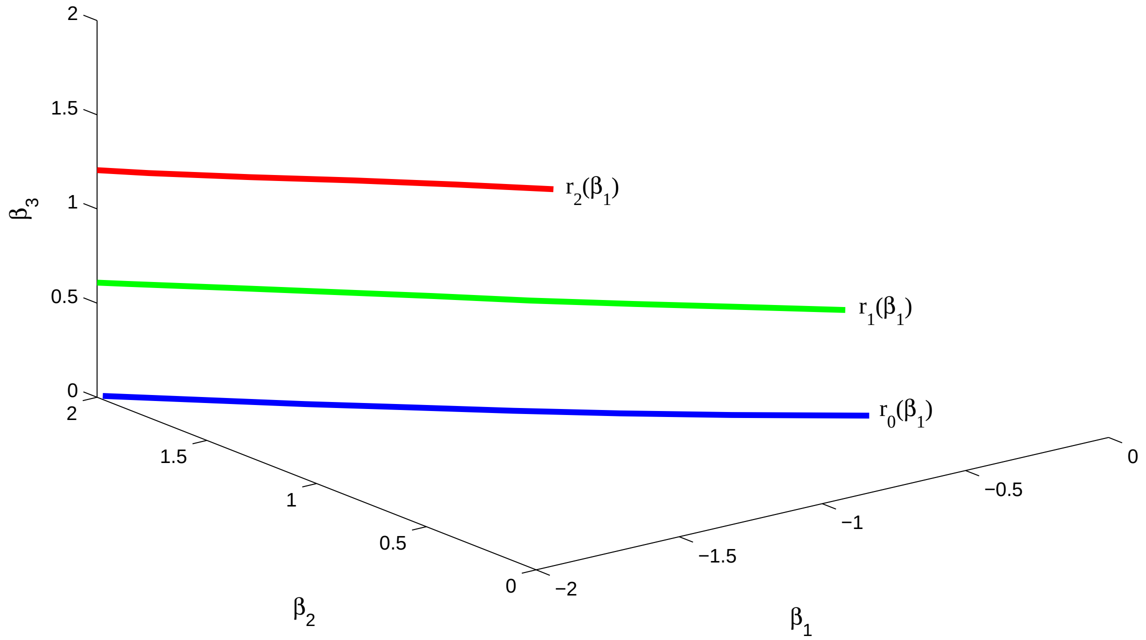

FIGURE 3. The phase transition curves $r(\beta_1)$ (corresponding to $\beta_3 = 0$, $\beta_3 = 1$, and $\beta_3 = 2$) in the $(\beta_1, \beta_2, \beta_3)$ space. Graph drawn for $p = 3$ and $q = 5$.

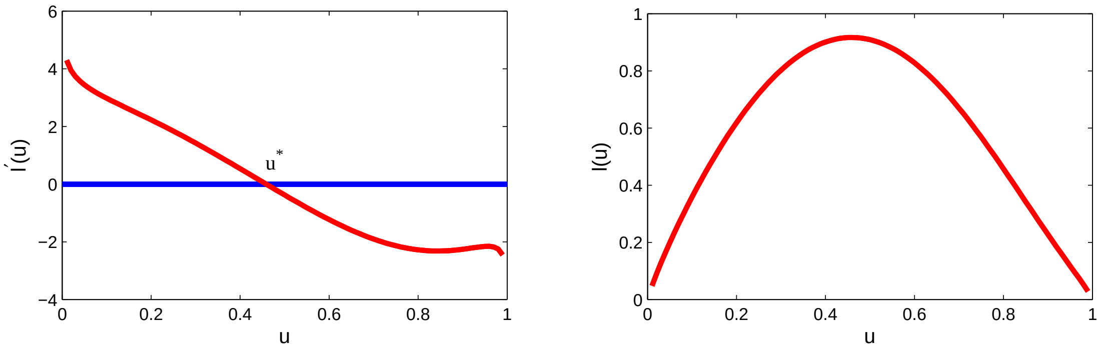

FIGURE 4. Outside the V-shaped region, $l_{\beta_3}(u)$ has a unique local maximizer (hence global maximizer) u^*. Graph drawn for $\beta_1 = 2$, $\beta_2 = -4$, $\beta_3 = 2$, $p = 3$, and $q = 5$.

Proof. The location of maximizers of $l_{\beta_3}(u)$ on the interval $[0,1]$ is closely related to the properties of its derivatives $l'_{\beta_3}(u)$ and $l''_{\beta_3}(u)$:

$$l'_{\beta_3}(u) = \beta_1 + p\beta_2 u^{p-1} + q\beta_3 u^{q-1} - \frac{1}{2}\log\frac{u}{1-u}, \tag{11}$$

$$l''_{\beta_3}(u) = p(p-1)\beta_2 u^{p-2} + q(q-1)\beta_3 u^{q-2} - \frac{1}{2u(1-u)}. \tag{12}$$

We first analyze the properties of $l''_{\beta_3}(u)$ on the interval $[0,1]$. Consider instead

$$F(u) = p(p-1)\beta_2 + q(q-1)\beta_3 u^{q-p} - \frac{1}{2u^{p-1}(1-u)}, \tag{13}$$

which is obtained by factorizing u^{p-2} out of $l''_{\beta_3}(u)$. Note that in doing so the effect of β_2 is minimized as varying β_2 only shifts the graph of $F(u)$ upward/downward and does not affect its shape. To examine the effect of β_3 on $F(u)$, we take one more derivative,

$$F'(u) = q(q-1)(q-p)\beta_3 u^{q-p-1} + \frac{(p-1)-pu}{2u^p(1-u)^2}. \tag{14}$$

Similarly as before, we factor u^{q-p-1} out of $F'(u)$ to minimize the effect of β_3. Let

$$f(u) = \frac{(p-1)-pu}{u^{q-1}(1-u)^2} \tag{15}$$

so that

$$F'(u) = \frac{1}{2}u^{q-p-1}(2q(q-1)(q-p)\beta_3 + f(u)). \tag{16}$$

We claim that the condition $2 \le p \le q \le 5p-1$ guarantees that $f(u)$ is monotonically decreasing on $[0,1]$. Independent of p and q, $f(0) = \infty$ and $f(1) = -\infty$. Its derivative $f'(u)$ is given by

$$f'(u) = -\frac{pqu^2 + (p+q+1-2pq)u + (p-1)(q-1)}{u^q(1-u)^3}. \tag{17}$$

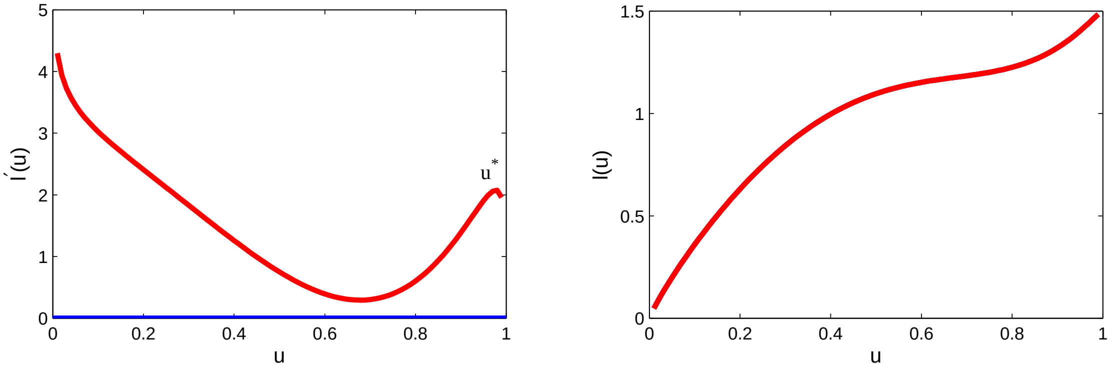

Figure 5. Outside the V-shaped region, $l_{\beta_3}(u)$ has a unique local maximizer (hence global maximizer) u^*. Graph drawn for $\beta_1 = 2$, $\beta_2 = -2.5$, $\beta_3 = 2$, $p = 3$, and $q = 5$.

Rearranging terms in the discriminant Δ of the numerator of $f'(u)$ yields a quadratic equation in q,

$$\Delta = q^2 + 2(1-3p)q + (p+1)^2 \tag{18}$$

with two zeros

$$q_{1,2} = (3p-1) \pm 2\sqrt{2(p^2-p)}. \tag{19}$$

We can easily check that $q_1 \le p$ and $q_2 \ge 5p-1$. As $q_1 \le q \le q_2$ is equivalent to $\Delta \le 0$, this verifies our claim.

An immediate corollary is that there is a unique u_0 in $(0,1)$ such that $F'(u_0) = 0$, with $F'(u) > 0$ for $u < u_0$, and $F'(u) < 0$ for $u > u_0$. The correspondence between β_3 and u_0 is one-to-one, and we may alternatively describe β_3 by

$$\beta_3 = \frac{pu_0 - (p-1)}{2q(q-1)(q-p)u_0^{q-1}(1-u_0)^2}. \tag{20}$$

This further implies that $F(u)$ is increasing from 0 to u_0, and decreasing from u_0 to 1, with the global maximum achieved at u_0,

$$F(u_0) = p(p-1)\beta_2 + \frac{qu_0 - (q-1)}{2(q-p)u_0^{p-1}(1-u_0)^2}. \tag{21}$$

Let

$$\beta_2^c = \frac{qu_0 - (q-1)}{2p(p-1)(p-q)u_0^{p-1}(1-u_0)^2} \tag{22}$$

so that $F(u_0; \beta_2^c) = 0$. As $F(u)$ and $l''_{\beta_3}(u)$ always carry the same sign, this shows that for $\beta_2 \le \beta_2^c$, $l''_{\beta_3}(u) \le 0$ on the whole interval $[0,1]$; whereas for $\beta_2 > \beta_2^c$, $l''_{\beta_3}(u)$ takes on both positive and negative values, and we denote the transition points by u_1 and u_2 ($u_1 < u_0 < u_2$), which are solely determined by β_2, and vice versa. Let

$$m(u) = \frac{1}{2p(p-1)u^{p-1}(1-u)} + \frac{(p-1) - pu_0}{2p(p-1)(q-p)u_0^{q-1}(1-u_0)^2}u^{q-p} \tag{23}$$

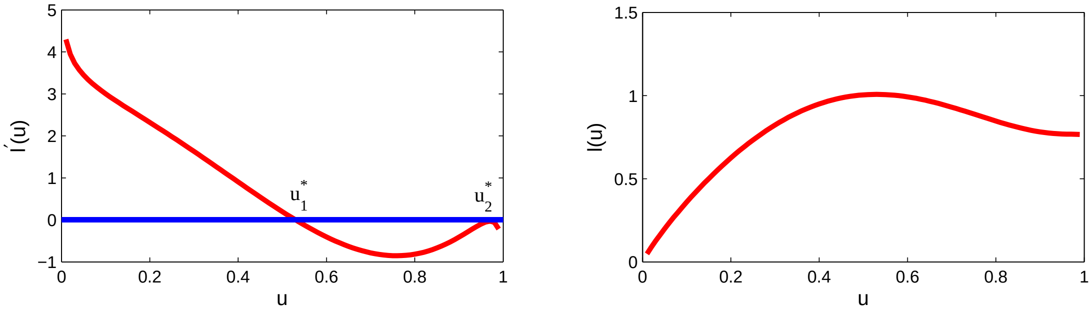

FIGURE 6. Along the lower bounding curve $m(b(\beta_1))$ of the V-shaped region, $l'_{\beta_3}(u)$ has two zeros u_1^* and u_2^*, but only u_1^* is the global maximizer for $l_{\beta_3}(u)$. Graph drawn for $\beta_1 = 2$, $\beta_2 = -3.24$, $\beta_3 = 2$, $p = 3$, and $q = 5$.

so that $\beta_2 = m(u_1) = m(u_2)$. As $m(u) = \beta_2 - F(u)/p(p-1)$, we have $m(0) = m(1) = \infty$, $m(u)$ is decreasing from 0 to u_0, and increasing from u_0 to 1.

Based on the properties of $l''_{\beta_3}(u)$, we next analyze the properties of $l'_{\beta_3}(u)$ on the interval $[0, 1]$. For $\beta_2 \leq \beta_2^c$, $l'_{\beta_3}(u)$ is monotonically decreasing. For $\beta_2 > \beta_2^c$, $l'_{\beta_3}(u)$ is decreasing from 0 to u_1, increasing from u_1 to u_2, then decreasing again from u_2 to 1. For reasons that will become clear in a moment, we write down the explicit expressions of $l'_{\beta_3}(u_1)$ and $l'_{\beta_3}(u_2)$:

$$l'_{\beta_3}(u_1) = \beta_1 + \frac{1}{2(p-1)(1-u_1)} - \frac{1}{2}\log\frac{u_1}{1-u_1} + \frac{(p-1)-pu_0}{2(p-1)(q-1)u_0^{q-1}(1-u_0)^2}u_1^{q-1}, \tag{24}$$

$$l'_{\beta_3}(u_2) = \beta_1 + \frac{1}{2(p-1)(1-u_2)} - \frac{1}{2}\log\frac{u_2}{1-u_2} + \frac{(p-1)-pu_0}{2(p-1)(q-1)u_0^{q-1}(1-u_0)^2}u_2^{q-1}. \tag{25}$$

Finally, based on the properties of $l'_{\beta_3}(u)$ and $l''_{\beta_3}(u)$, we analyze the properties of $l_{\beta_3}(u)$ on the interval $[0, 1]$. Independent of p and q, $l_{\beta_3}(u)$ is a bounded continuous function, $l'_{\beta_3}(0) = \infty$, and $l'_{\beta_3}(1) = -\infty$, so $l_{\beta_3}(u)$ can not be maximized at 0 or 1. For $\beta_2 \leq \beta_2^c$, $l'_{\beta_3}(u)$ crosses the u-axis only once, going from positive to negative. Thus $l_{\beta_3}(u)$ has a unique local maximizer (hence global maximizer) u^*. For $\beta_2 > \beta_2^c$, the situation is more complicated. If $l'_{\beta_3}(u_1) \geq 0$ (resp. $l'_{\beta_3}(u_2) \leq 0$), $l_{\beta_3}(u)$ has a unique local maximizer (hence global maximizer) at a point $u^* > u_2$ (resp. $u^* < u_1$). If $l'_{\beta_3}(u_1) < 0 < l'_{\beta_3}(u_2)$, then $l_{\beta_3}(u)$ has two local maximizers u_1^* and u_2^*, with $u_1^* < u_1 < u_0 < u_2 < u_2^*$ (see Figures 4 and 5).

Let

$$n(u) = \frac{1}{2(p-1)(1-u)} - \frac{1}{2}\log\frac{u}{1-u} + \frac{(p-1)-pu_0}{2(p-1)(q-1)u_0^{q-1}(1-u_0)^2}u^{q-1} \tag{26}$$

so that $l'_{\beta_3}(u_1) = \beta_1 + n(u_1)$ and $l'_{\beta_3}(u_2) = \beta_1 + n(u_2)$. Independent of p and q, $n(0) = \infty$ and $n(1) = \infty$. Its derivative $n'(u)$ is given by

$$\begin{aligned} n'(u) &= \frac{1}{2(p-1)}u^{q-2}\left(\frac{(p-1)-pu_0}{u_0^{q-1}(1-u_0)^2} - \frac{(p-1)-pu}{u^{q-1}(1-u)^2}\right) \\ &= \frac{1}{2(p-1)}u^{q-2}\left(f(u_0) - f(u)\right). \end{aligned} \tag{27}$$

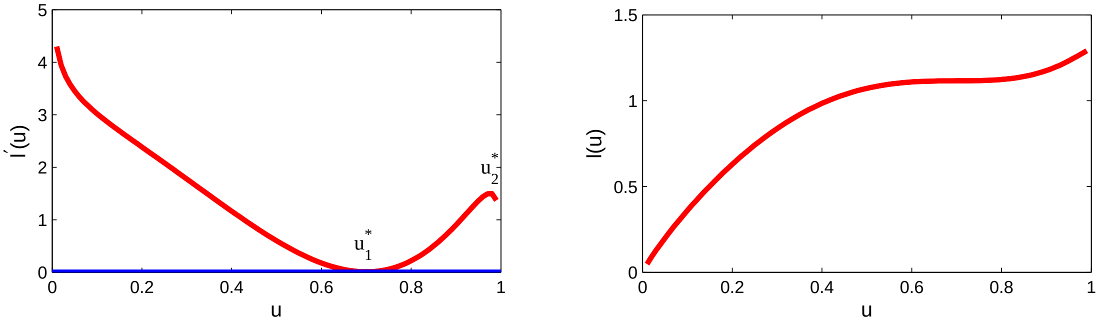

FIGURE 7. Along the upper bounding curve $m(a(\beta_1))$ of the V-shaped region, $l'_{\beta_3}(u)$ has two zeros u_1^* and u_2^*, but only u_2^* is the global maximizer for $l_{\beta_3}(u)$. Graph drawn for $\beta_1 = 2$, $\beta_2 = -2.7$, $\beta_3 = 2$, $p = 3$, and $q = 5$.

As $f(u)$ is monotonically decreasing, $n(u)$ is decreasing from 0 to u_0, and increasing from u_0 to 1, with the global minimum achieved at u_0,

$$n(u_0) = \frac{1}{2(p-1)(1-u_0)} - \frac{1}{2}\log\frac{u_0}{1-u_0} + \frac{(p-1)-pu_0}{2(p-1)(q-1)(1-u_0)^2}. \tag{28}$$

This implies that $l'_{\beta_3}(u_1;\beta_1,\beta_2^c) \geq 0$ for

$$\beta_1 \geq \beta_1^c = \frac{1}{2}\log\frac{u_0}{1-u_0} - \frac{1}{2(p-1)(1-u_0)} + \frac{pu_0-(p-1)}{2(p-1)(q-1)(1-u_0)^2}. \tag{29}$$

The only possible region in the (β_1,β_2) plane where $l'_{\beta_3}(u_1) < 0 < l'_{\beta_3}(u_2)$ is thus bounded by $\beta_1 < \beta_1^c$ and $\beta_2 > \beta_2^c$.

We now analyze the behavior of $l'_{\beta_3}(u_1)$ and $l'_{\beta_3}(u_2)$ more closely when β_1 and β_2 are chosen from this region. Recall that $u_1 < u_0 < u_2$. By monotonicity of $n(u)$ on the intervals $(0,u_0)$ and $(u_0,1)$, there exist continuous functions $a(\beta_1)$ and $b(\beta_1)$ of β_1, such that $l'_{\beta_3}(u_1) < 0$ for $u_1 > a(\beta_1)$ and $l'_{\beta_3}(u_2) > 0$ for $u_2 > b(\beta_1)$. As $\beta_1 \to -\infty$, $a(\beta_1) \to 0$ and $b(\beta_1) \to 1$. $a(\beta_1)$ is an increasing function of β_1, whereas $b(\beta_1)$ is a decreasing function, and they satisfy

$$n(a(\beta_1)) = n(b(\beta_1)) = -\beta_1. \tag{30}$$

The restrictions on u_1 and u_2 yield restrictions on β_2, and we have $l'_{\beta_3}(u_1) < 0$ for $\beta_2 < m(a(\beta_1))$ and $l'_{\beta_3}(u_2) > 0$ for $\beta_2 > m(b(\beta_1))$. As $\beta_1 \to -\infty$, $m(a(\beta_1)) \to \infty$ and $m(b(\beta_1)) \to \infty$. $m(a(\beta_1))$ and $m(b(\beta_1))$ are both decreasing functions of β_1, and they satisfy

$$l'_{\beta_3}(u_1;\beta_1,m(a(\beta_1))) = l'_{\beta_3}(u_2;\beta_1,m(b(\beta_1))) = 0. \tag{31}$$

As $l'_{\beta_3}(u_2;\beta_1,\beta_2) > l'_{\beta_3}(u_1;\beta_1,\beta_2)$ for every (β_1,β_2), the curve $m(b(\beta_1))$ must lie below the curve $m(a(\beta_1))$, and together they generate the bounding curves of the V-shaped region in the (β_1,β_2) plane with corner point (β_1^c,β_2^c) where two local maximizers exist for $l_{\beta_3}(u)$ (see Figures 6 and 7).

Fix an arbitrary $\beta_1 < \beta_1^c$, we examine the effect of varying β_2 on the graph of $l'_{\beta_3}(u)$. It is clear that $l'_{\beta_3}(u)$ shifts upward as β_2 increases and downward as β_2 decreases. As a result, as β_2 gets large, the positive area bounded by the curve $l'_{\beta_3}(u)$ increases, whereas the negative area decreases. By the fundamental theorem of calculus, the difference between the positive

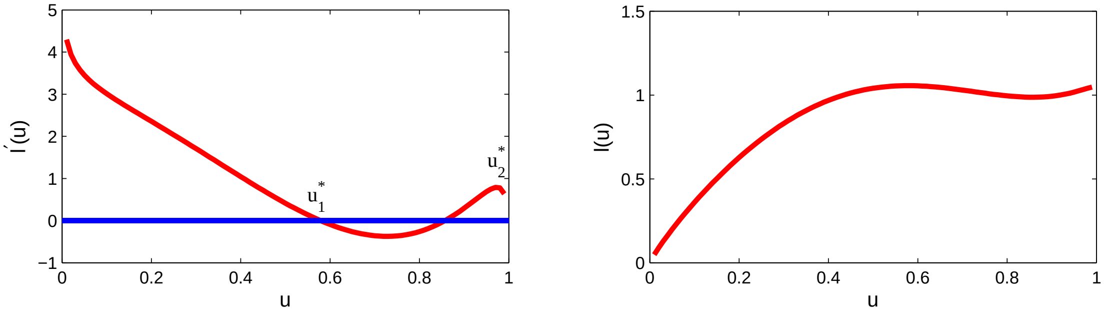

FIGURE 8. Along the phase transition curve $r(\beta_1)$, $l_{\beta_3}(u)$ has two local maximizers u_1^* and u_2^*, and both are global maximizers for $l_{\beta_3}(u)$. Graph drawn for $\beta_1 = 2$, $\beta_2 = -2.95$, $\beta_3 = 2$, $p = 3$, and $q = 5$.

and negative areas is the difference between $l_{\beta_3}(u_2^*)$ and $l_{\beta_3}(u_1^*)$, which goes from negative ($l'_{\beta_3}(u_2) = 0$, u_1^* is the global maximizer) to positive ($l'_{\beta_3}(u_1) = 0$, u_2^* is the global maximizer) as β_2 goes from $m(b(\beta_1))$ to $m(a(\beta_1))$. Thus there must be a unique $\beta_2 : m(b(\beta_1)) < \beta_2 < m(a(\beta_1))$ such that u_1^* and u_2^* are both global maximizers, and we denote this β_2 by $r_{\beta_3}(\beta_1)$ (see Figure 8). The parameter values of $(\beta_1, r_{\beta_3}(\beta_1))$ are exactly the ones for which positive and negative areas bounded by $l'_{\beta_3}(u)$ equal each other. An increase in β_1 induces an upward shift of $l'_{\beta_3}(u)$, and must be balanced by a decrease in β_2. Similarly, a decrease in β_1 induces a downward shift of $l'_{\beta_3}(u)$, and must be balanced by an increase in β_2. This justifies that r_{β_3} is monotonically decreasing in β_1. □

Corollary 2.2 (Universality). *Fix* $\beta_3 \geq 0$. *The transition curve* $\beta_2 = r_{\beta_3}(\beta_1)$ *displays a universal asymptotic behavior as* $\beta_1 \to -\infty$*:*

$$\lim_{\beta_1 \to -\infty} |r_{\beta_3}(\beta_1) + \beta_1 + \beta_3| = 0. \tag{32}$$

Proof. By Proposition 2.1, it suffices to show that as $\beta_1 \to -\infty$, $l_{\beta_3}(u; \beta_1, -\beta_1 - \beta_3)$ has two global maximizers u_1^* and u_2^*. This is easy when we realize that as $\beta_1 \to -\infty$, $l_{\beta_3}(u; \beta_1, -\beta_1 - \beta_3) \to -\infty$ for every u in $(0, 1)$. The limiting maximizers on $[0, 1]$ are thus $u_1^* = 0$ and $u_2^* = 1$, with $l_{\beta_3}(u_1^*) = l_{\beta_3}(u_2^*) = 0$. □

Proposition 2.3. *As* $\beta_3 \geq 0$ *varies, the transition curves* $\beta_2 = r_{\beta_3}(\beta_1)$ *(subject to* $\beta_2 \geq 0$*) trace out a continuous surface* S *with three bounding curves* C_1*,* C_2*, and* C_3*.*

Proof. The continuity of the transition surface S follows easily once we realize that it consists exactly of parameter values of $(\beta_1, \beta_2, \beta_3)$ for which $l_{\beta_3}(u)$ (continuous in β_1, β_2, and β_3) has two global maximizers. By Corollary 2.2, S displays a universal asymptotic behavior: As $\beta_1 \to -\infty$, $\beta_2 \to \infty$, and $\beta_3 \to \infty$, the distance between S and the plane $\beta_1 + \beta_2 + \beta_3 = 0$ shrinks to zero. Due to the non-negativity constraints on β_2 and β_3, S is bounded by three curves C_1, C_2, and C_3: The curve C_1 is the intersection of S with the (β_1, β_2) plane, and is given by $\beta_2 = r_0(\beta_1)$ (cf. Proposition 2.1); The curve C_2 is the intersection of S with the (β_1, β_3) plane, and is given analogously (with p and q switched in (8)); The curve C_3 is a critical curve, and is traced out by the critical points (β_1^c, β_2^c) (9) (subject to $\beta_2^c \geq 0$). □

3. Critical Behavior

By Propositions 2.1 and 2.3, the maximization problem (8) is solved at a unique value u^* off S, and at two values u_1^* and u_2^* on S (the jump from u_1^* to u_2^* is quite noticeable even for small parameter values of β). Thus by Theorems 1.4 and 1.5, in the large n limit, a typical G_n drawn from (1) is indistinguishable from the Erdős-Rényi graph $G(n,u^*)$ off the transition surface S, however, on the transition surface S, the structure of G_n is not completely deterministic: It may behave like an Erdős-Rényi graph $G(n,u_1^*)$, or it may behave like an Erdős-Rényi graph $G(n,u_2^*)$. Since the limiting free energy density ψ_∞^β encodes important information about the local features of the random graph G_n (see for example (4) and (5)), a thorough study of its analyticity properties is fundamental to understanding the global structure of the exponential model. The following theorems 3.1 and 3.3 are dedicated to this goal. Together they complete the proof of our main theorem (Theorem 1.2).

Theorem 3.1. *Consider a* 3*-parameter exponential random graph model (1). Assume* H_2 *has* p *edges and* H_3 *has* q *edges with* $2 \le p \le q \le 5p-1$*. Then the limiting free energy density* ψ_∞^β *is not an analytic function on the transition surface* S*.*

Proof. Due to the jump between the two solutions u_1^* and u_2^* of the maximization problem (8), all the first derivatives $\frac{\partial}{\partial\beta_1}\psi_\infty^\beta$, $\frac{\partial}{\partial\beta_2}\psi_\infty^\beta$, and $\frac{\partial}{\partial\beta_3}\psi_\infty^\beta$ have (jump) discontinuities across the transition surface S, except along the critical curve C_3:

$$\lim_{n\to\infty}\mathbb{E}^\beta t(H_1,G_n)=\lim_{n\to\infty}\mathbb{E}^\beta t(H_1,G(n,u^*))=u^*=\frac{\partial}{\partial\beta_1}\psi_\infty^\beta, \tag{33}$$

$$\lim_{n\to\infty}\mathbb{E}^\beta t(H_2,G_n)=\lim_{n\to\infty}\mathbb{E}^\beta t(H_2,G(n,u^*))=(u^*)^p=\frac{\partial}{\partial\beta_2}\psi_\infty^\beta, \tag{34}$$

$$\lim_{n\to\infty}\mathbb{E}^\beta t(H_3,G_n)=\lim_{n\to\infty}\mathbb{E}^\beta t(H_3,G(n,u^*))=(u^*)^q=\frac{\partial}{\partial\beta_3}\psi_\infty^\beta. \tag{35}$$

To see that the transition across C_3 is second-order, we check the first and second derivatives of ψ_∞^β in the neighborhood of this curve. By Proposition 2.1, for every $(\beta_1^c,\beta_2^c,\beta_3)$ on C_3, $l'_{\beta_3}(u;\beta_1^c,\beta_2^c)$ is monotonically decreasing on $[0,1]$, and the unique zero is achieved at u_0 (10). Take any $0<\epsilon<\min\{u_0,1-u_0\}$. Set $\delta=\min\{l'_{\beta_3}(u_0-\epsilon),-l'_{\beta_3}(u_0+\epsilon)\}$. Consider $(\bar\beta_1,\bar\beta_2,\bar\beta_3)$ so close to $(\beta_1^c,\beta_2^c,\beta_3)$ such that $|\bar\beta_1-\beta_1^c|+p|\bar\beta_2-\beta_2^c|+q|\bar\beta_3-\beta_3|<\delta$. For every u in $[0,1]$, we then have $\left|l'_{\beta_3}(u;\bar\beta_1,\bar\beta_2)-l'_{\beta_3}(u;\beta_1^c,\beta_2^c)\right|<\delta$. It follows that the zero $u^*(\bar\beta_1,\bar\beta_2,\bar\beta_3)$ (or u_1^* and u_2^*) must satisfy $|u^*-u_0|<\epsilon$, which easily implies the continuity of $\frac{\partial}{\partial\beta_1}\psi_\infty^\beta$, $\frac{\partial}{\partial\beta_2}\psi_\infty^\beta$, and $\frac{\partial}{\partial\beta_3}\psi_\infty^\beta$ at $(\beta_1^c,\beta_2^c,\beta_3)$. Concerning the divergence of the second derivatives, we compute

$$\frac{\partial^2}{\partial\beta_1^2}\psi_\infty^\beta=\frac{\partial}{\partial\beta_1}u^*=-\frac{1}{l''_{\beta_3}(u^*)},\qquad \frac{\partial^2}{\partial\beta_2^2}\psi_\infty^\beta=\frac{\partial}{\partial\beta_2}(u^*)^p=-\frac{p^2(u^*)^{2p-2}}{l''_{\beta_3}(u^*)}, \tag{36}$$

$$\frac{\partial^2}{\partial\beta_3^2}\psi_\infty^\beta=\frac{\partial}{\partial\beta_3}(u^*)^q=-\frac{q^2(u^*)^{2q-2}}{l''_{\beta_3}(u^*)},\qquad \frac{\partial^2}{\partial\beta_1\partial\beta_2}\psi_\infty^\beta=\frac{\partial}{\partial\beta_1}(u^*)^p=-\frac{p(u^*)^{p-1}}{l''_{\beta_3}(u^*)}, \tag{37}$$

$$\frac{\partial^2}{\partial\beta_1\partial\beta_3}\psi_\infty^\beta=\frac{\partial}{\partial\beta_1}(u^*)^q=-\frac{q(u^*)^{q-1}}{l''_{\beta_3}(u^*)},\qquad \frac{\partial^2}{\partial\beta_2\partial\beta_3}\psi_\infty^\beta=\frac{\partial}{\partial\beta_2}(u^*)^q=-\frac{pq(u^*)^{p+q-2}}{l''_{\beta_3}(u^*)}. \tag{38}$$

But as was explained in Proposition 2.1, as $(\bar{\beta}_1, \bar{\beta}_2, \bar{\beta}_3)$ approaches C_3, $l''_{\bar{\beta}_3}(u^*; \bar{\beta}_1, \bar{\beta}_2)$ converges to zero. The desired singularity is thus justified. ☐

Real and complex analyticity are both defined in terms of convergent power series. To examine the analyticity of the limiting free energy density ψ_∞^β off the transition surface S, we resort to an analytic implicit function theorem, which may be interpreted in either the real or the complex setting.

Theorem 3.2 (Krantz-Parks [18])**.** *Suppose that the power series*

$$F(x,y) = \sum_{\alpha,k} a_{\alpha,k} x^\alpha y^k \tag{39}$$

is absolutely convergent for $|x| \leq R_1$ *and* $|y| \leq R_2$*. If* $a_{0,0} = 0$ *and* $a_{0,1} \neq 0$*, then there exist* $r_0 > 0$ *and a power series*

$$f(x) = \sum_{|\alpha|>0} c_\alpha x^\alpha \tag{40}$$

such that (40) is absolutely convergent for $|x| \leq r_0$ *and* $F(x, f(x)) = 0$*.*

Theorem 3.3. *Consider a 3-parameter exponential random graph model (1). Suppose* β_2 *and* β_3 *are non-negative. Assume* H_2 *has* p *edges and* H_3 *has* q *edges with* $2 \leq p \leq q \leq 5p-1$*. Then the limiting free energy density* ψ_∞^β *is an analytic function off the transition surface* S*.*

Proof. It is clear that $l_{\beta_3}(u; \beta_1, \beta_2)$ is analytic for $u \in (0,1)$, $\beta_1 \in (-\infty, \infty)$, $\beta_2 \in (-\infty, \infty)$, and $\beta_3 \in (-\infty, \infty)$. We show that the maximizer u^* for $l_{\beta_3}(u; \beta_1, \beta_2)$ is an analytic function of β off the transition surface S. Fix $(\beta_1, \beta_2, \beta_3)$ not on S. For $(\bar{\beta}_1, \bar{\beta}_2, \bar{\beta}_3)$ close to $(\beta_1, \beta_2, \beta_3)$, we transform the function $l'_{\bar{\beta}_3}(u; \bar{\beta}_1, \bar{\beta}_2)$ into a function $F(x,y)$ by setting $x = (\bar{\beta}_1 - \beta_1, \bar{\beta}_2 - \beta_2, \bar{\beta}_3 - \beta_3)$ and $y = u - u^*(\beta_1, \beta_2, \beta_3)$. It is easy to check that $F(x,y)$ satisfies all the conditions of Theorem 3.2: It has the desired domain of analyticity, is locally absolutely convergent, and its first two coefficients are given by

$$a_{0,0} = F(0,0) = l'_{\beta_3}(u^*(\beta_1, \beta_2, \beta_3); \beta_1, \beta_2) = 0, \tag{41}$$

$$a_{0,1} = \frac{\partial F}{\partial y}(0,0) = l''_{\beta_3}(u^*(\beta_1, \beta_2, \beta_3); \beta_1, \beta_2) \neq 0. \tag{42}$$

The absolute convergence for $f(x) = u^*(\bar{\beta}_1, \bar{\beta}_2, \bar{\beta}_3) - u^*(\beta_1, \beta_2, \beta_3)$ then follows easily, which implies the analyticity of u^* as a function of β. As the composition of analytic functions is analytic as long as the domain and range match up, by Theorem 1.4, this further implies the analyticity of $\psi_\infty^\beta = l_{\beta_3}(u^*; \beta_1, \beta_2)$ as a function of β off the transition surface S, where the maximizer u^* is uniquely defined. ☐

ACKNOWLEDGEMENTS

The author gratefully acknowledges the support of the National Science Foundation through two international travel grants, which enabled her to attend the 8th World Congress on Probability and Statistics and the 17th International Congress on Mathematical Physics, where she had the opportunity to discuss this work.

References

[1] Besag, J.: Statistical analysis of non-lattice data. J. Roy. Statist. Soc. Ser. D 24, 179-195 (1975)

[2] Hammersley, J., Clifford, P.: Markov fields on finite graphs and lattices. http://www.statslab.cam.ac.uk/˜ grg/books/hammfest/hamm-cliff.pdf (1971)

[3] Holland, P., Leinhardt, S.: An exponential family of probability distributions for directed graphs. J. Amer. Statist. Assoc. 76, 33-50 (1981)

[4] Frank, O., Strauss, D.: Markov graphs. J. Amer. Statist. Assoc. 81, 832-842 (1986)

[5] Snijders, T., Pattison, P., Robins, G., Handcock M.: New specifications for exponential random graph models. Sociol. Method. 36, 99-153 (2006)

[6] Rinaldo, A., Fienberg, S., Zhou, Y.: On the geometry of discrete exponential families with application to exponential random graph models. Electron. J. Stat. 3, 446-484 (2009)

[7] Wasserman, S., Faust, K.: Social Network Analysis: Methods and Applications. Cambridge University Press, Cambridge (2010)

[8] Yang, C.N., Lee, T.D.: Statistical theory of equations of state and phase transitions. Phys. Rev. 87, 404-419 (1952)

[9] Erdős, P., Rényi, A.: On the evolution of random graphs. Publ. Math. Inst. Hung. Acad. Sci. 5, 17-61 (1960)

[10] Park, J., Newman, M.: Solution of the two-star model of a network. Phys. Rev. E 70, 066146 (2004)

[11] Park, J., Newman, M.: Solution for the properties of a clustered network. Phys. Rev. E 72, 026136 (2005)

[12] Chatterjee, S., Diaconis, P.: Estimating and understanding exponential random graph models. arXiv: 1102.2650v3 (2011)

[13] Lovász, L., Szegedy B.: Limits of dense graph sequences. J. Combin. Theory Ser. B 96, 933-957 (2006)

[14] Häggström, O., Jonasson, J.: Phase transition in the random triangle model. J. Appl. Probab. 36, 1101-1115 (1999)

[15] Bhamidi, S., Bresler, G., Sly, A.: Mixing time of exponential random graphs. Ann. Appl. Probab. 21, 2146-2170 (2011)

[16] Radin, C., Yin, M.: Phase transitions in exponential random graphs. arXiv: 1108.0649v2 (2011)

[17] Aristoff, D., Radin, C.: Emergent structures in large networks. arXiv: 1110.1912v1 (2011)

[18] Krantz, S., Parks, H.: The Implicit Function Theorem: History, Theory, and Applications. Birkhäuser, Boston (2002)

DEPARTMENT OF MATHEMATICS, UNIVERSITY OF TEXAS, AUSTIN, TX, 78712, USA
E-mail address: `myin@math.utexas.edu`